World Academy of Science, Engineering and Technology
International Journal of Mechanical and Mechatronics Engineering
Vol:15, No:1, 2021

Modal Analysis of a Cantilever Beam Using an Inexpensive Smartphone Camera: Motion Magnification Technique

Hasan Hassoun, Jaafar Hallal, Denis Duhamel, Mohammad Hammoud, Ali Hage Diab

***Abstract*—**This paper aims to prove the accuracy of an inexpensive smartphone camera as a non-contact vibration sensor to recover the vibration modes of a vibrating structure such as a cantilever beam. A video of a vibrating beam is filmed using a smartphone camera and then processed by the motion magnification technique. Based on this method, the first two natural frequencies and their associated mode shapes are estimated experimentally and compared to the analytical ones. Results show a relative error of less than 4% between the experimental and analytical approaches for the first two natural frequencies of the beam. Also, for the first two-mode shapes, a Modal Assurance Criterion (MAC) value of above 0.9 between the two approaches is obtained. This slight error between the different techniques ensures the viability of a cheap smartphone camera as a non-contact vibration sensor, particularly for structures vibrating at relatively low natural frequencies.

***Keywords*—**Modal Analysis, motion magnification, smartphone camera, structural vibration, vibration modes.

I. Introduction

VIBRATION response of any structure depends on its material properties and geometrical shape in addition to the excitation force characteristics such as the frequency, amplitude, direction and the point of application. The modal characteristics of a vibrating structure can be determined based on modal analysis. The end goal of the modal analysis is to collect data from the vibrating structure to characterize its vibrational behavior. Experimental modal analysis can be performed using contact methods such as with accelerometers or non-contact methods using laser vibrometry. Contact sensors such as accelerometers are used for modal analysis with high accuracy [1]. However, this type of sensors affects the obtained results due to its mass especially when used for small structures, in addition to the difficulty and numerous sensors when used for large structures. Noncontact sensors such as laser vibrometry [2], [3] depend on the electromagnetic radiation to transmit data, but it is expensive. This later sensor measures the velocity at a discrete point using a focused laser beam. The velocity is then calculated using the Doppler shift between the incidents light and scattered light returning to the measuring device.

A modern approach called motion magnification based on processing the time series of the vibration response or color values in the video at each pixel was recently used. This is achieved by applying a signal processing to each time series to amplify a band of interesting frequencies between the low and high cutoff frequencies. This modern method provides a promising technique for visualizing and obtaining small displacements [4]-[7]. This methodology, firstly developed by MIT [8], was used to estimate the material properties of an object in addition to the vibration modes of a rod using an expensive camera [9], structural damage identification [10], and to recover sound from the video [11]. Different fields of use exist such as for medical purposes where the periodic motion of the head due to the movement of blood [12] is detected. Extraction of features using video cameras provides an interesting and promising method for modal analysis of a vibrating structure. They can be employed as inspection sensors or remote monitoring. These video cameras range from expensive and precise instruments with a high-resolution and large frame rate to inexpensive equipment such as a smartphone camera.

The motion magnification technique was applied successfully in different fields, but it uses expensive cameras with a large frame rate. However, the presented work aims to ensure the feasibility of an inexpensive smartphone camera as a non-contact vibration sensor.

This paper is organized as follows: Section II presents the analytical calculation used to determine the natural frequencies of a cantilever beam. Besides, this section presents the motion magnification methodology applied on a vibrating beam using an inexpensive smartphone camera. Section III validates the experimental results from the motion magnification technique by comparing the extracted modes to the analytical ones. A conclusion and suggestions for future work will be presented in Section IV.

II. Methodology

The feasibility of an inexpensive smartphone camera as a vibration sensor for modal identification will be examined by recovering the first two vibration modes experimentally based on motion magnification technique and compared to the analytical ones. This section presents first the analytical model of the cantilever beam. Then, the motion magnification technique will be discussed to present how qualitative features

Hasan Hassoun is with Navier Laboratory, Ecole des Ponts ParisTech, Champs sur Marne, France (corresponding author, phone: +33753634711; e-mail: hasan.hassoun@enpc.fr).

Jaafar Hallal, Mohammad Hammoud and Ali Hage Diab are with Department of Engineering, Lebanese International University, Lebanon (e-mail: Jaafar.hallal@liu.edu.lb, mohamad.hammoud@liu.edu.lb, ali.hagediab@liu.edu.lb).

Denis Duhamel is with Navier Laboratory, Ecole des Ponts ParisTech, Champs sur Marne, France (e-mail: denis.duhamel@enpc.fr).

inside the video can be analyzed to extract the beam mode shapes and their corresponding natural frequencies. The dimensions and material properties of the used beam model are shown in Table I.

TABLE I
BEAM SPECIFICATIONS

Symbol	Quantity	SI[a] Unit
E	elastic modulus	2×10^{11} Pa
ρ	density	7870 Kg/m^3
l	length	0.419 m
b	width	0.0294 m
h	thickness	0.00103 m

[a]SI units are the International system of units; Pa = Pascal, kg = kilogram, m = meter.

A. Analytical Modeling

A cantilever beam is a structure used in many practical engineering applications such as vibration absorbers and turbine blades. The vibration of the beam is studied in the transverse direction applying Euler-Bernoulli theory since l/b = 14.25 and l/h = 406.8 > 10. Fig. 1 illustrates a cantilever beam under transverse vibration (the deflection w(x,t) is in the y-direction). The presented cantilever beam has a rectangular cross-section A, width b, thickness h, length l, and bending stiffness EI (E is Young's modulus and I is the cross-sectional area moment of inertia about the z-axis).

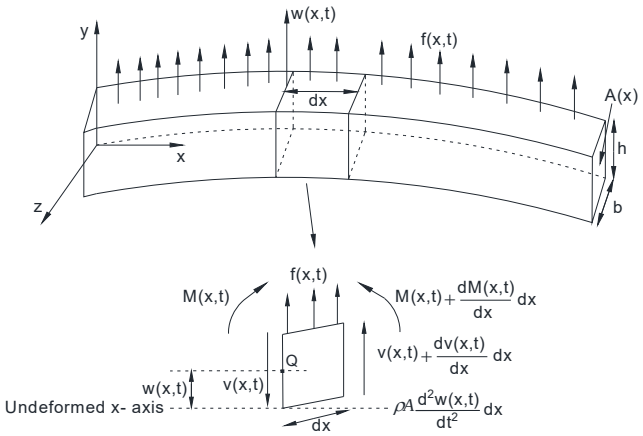

Fig. 1 Free body diagram of a transverse cross-section of a cantilever beam

The formulation procedure of the undamped natural frequency equation can be obtained from the beam free vibration behavior (f (x,t) = 0), which can be written as:

$$EI\,\frac{\partial^4 w(x,t)}{\partial x^4} + \rho A\,\frac{\partial^2 w(x,t)}{\partial t^2} = 0 \tag{1}$$

Equation (1) can be solved by considering four boundary conditions since the derived equation contains four spatial derivatives. It will not be reviewed in this work as it can be found in [15]. The obtained undamped natural frequencies (ω_i) are related directly to the material properties and the geometrical parameters by:

$$\omega_i = k^2\sqrt{\frac{Eh^2}{12\,\rho l^4}} \tag{2}$$

Parameter k depends on the mode number. The first five natural frequencies are calculated by substituting the values of the constant k by 1.87, 4.69, 7.85, 10.99 and 14.13, respectively. For the rest of modes (i.e., for values of n > 5), natural resonant frequencies can be obtained by computing the parameter k using $k = \frac{(2n-1)}{2}\pi$.

B. Motion Magnification Technique

Motion magnification is an algorithm for extraction features of a vibrating object inside the video. A video consists of a series of images which has two domains: First, the time domain corresponding to the number of images that make the video and second the spatial domain corresponding to a 2D field of brightness value in an image. These images can be decomposed in the spatial domain by filters into phase and amplitude signals to form a time-varying signals representative of the video.

Based on the phase-based motion magnification [16], the displacement signal of the vibrating object inside the video can be estimated in the time domain (In this case the vibrating object is a cantilever beam). Once the displacement signal is obtained, the Fourier transform is used to transform the displacement signal from the time domain into the frequency domain. The peaks in the Fourier spectrum of the displacement signal correspond to the modal frequencies (natural frequencies). These modal frequencies do not vary across the surface of the structure in which the power spectra of local motions should have peaks at the same resonant frequencies. Therefore, the global motion power spectrum can be computed for a video by averaging the local motion power spectra extracted at every pixel. This leads to a signal temporal power spectrum describing the modal frequencies of motion that exist in the filmed video. Once the modal frequencies are obtained, the spatially varying displacement signal in the video is filtered with a bandpass filter centered at each modal frequency and with specified boundaries known as low and high cutoff frequencies. Thus, the obtained filtered displacement signal can be utilized to estimate the mode shape at its corresponding modal frequency.

1. Derivation

This technique is based on local phase and local amplitude in oriented bandpass filters [17], [18]. These are analogous quantities to the phase and amplitude of Fourier series coefficients, in which the phase controls the location of basis function while the amplitude controls its strength. The phase corresponds to global motion in case of Fourier transform while local phase gives a way to compute the local motion. Consider a video, with image brightness I(x,y,t) at spatial location (x,y) and time t, the local phase and local amplitude in orientation θ at a frame at time t_0 can be computed by a spatial bandpassing the frame with a complex filter $G_2^\theta + iH_2^\theta$ to get [4]:

$$A_\theta(x,y,t_0)e^{i\phi_\theta(x,y,t_0)} = \left(G_2^\theta + iH_2^\theta\right) \otimes I(x,y,t_0) \quad (3)$$

where $A_\theta(x,y,t_0)$ is the local amplitude, $\emptyset_\theta(x,y,t_0)$ is the local phase, G_2^θ and H_2^θ are steerable filters [19]. However, the constant contours of the local phase through time correspond to the displacement signal [17], [18]. This can be expressed as:

$$\phi_0(x,y,t) = c \quad (4)$$

By differentiating with respect to time, this yields to:

$$\left(\frac{\partial\phi_\theta(x,y,t)}{\partial x}, \frac{\partial\phi_\theta(x,y,t)}{\partial y}, \frac{\partial\phi_\theta(x,y,t)}{\partial t}\right).(u,v,1) = 0 \quad (5)$$

where u and v are the velocity in x and y directions respectively. Considering the case $\frac{\partial\emptyset_\theta(x,y,t)}{\partial y} \approx 0$ and $\frac{\partial\emptyset_{\pi/2}(x,y,t)}{\partial x} \approx 0$ [6], the velocity in units of a pixel can be expressed as:

$$u = -\left(\frac{\partial\phi_\theta(x,y,t)}{\partial x}\right)^{-1} \frac{\partial\phi_\theta(x,y,t)}{\partial t} \quad (6)$$

$$v = -\left(\frac{\partial\phi_{\pi/2}(x,y,t)}{\partial y}\right)^{-1} \frac{\partial\phi_{\pi/2}(x,y,t)}{\partial t} \quad (7)$$

The velocity between the first frame and the ith frame is computed to obtain the displacement signal in time. The displacement signal is converted to millimeters unit by multiplying the length of the structure in the scene divided by the number of pixels it spans. The result of mentioned processing is the time-domain displacement signal which can be transformed into the frequency domain by Fourier transform to obtain the modal frequencies.

2. Video Capture

To visualize the structure vibration modes, an appropriate frame rate is needed to treat these frequencies with the Nyquist limit [4]. This limit indicates that the wave frequency must not exceed half the sampling frequency. Besides, the video must be captured with enough time. For low frequencies, the captured video is long compared to that of high frequency. Note that filming with a higher fps will only expand the frequency range to recover higher modes but will not improve the accuracy unless the resolution is changed.

3. Experimental Measurement

The cantilever beam was clamped to a steel base next to two loudspeakers and excited by a white sound signal (Fig. 2). This excitation is stopped before filming so that the beam vibrates at its natural frequencies. The motion of the excited cantilever beam was filmed using the Samsung S9 smartphone camera at 240 fps (frame per second) in a closed room with no AC powered lights. With this latter fps filming, the camera will ensure recovering the modes below 120 Hz (240 fps/2). The specifications of the used camera are shown in Table II.

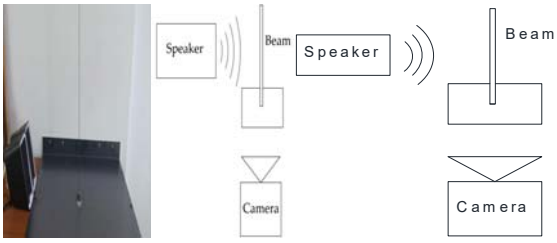

Fig. 2 Setup of the experimental measurement

TABLE II
SAMSUNG S9 SMARTPHONE CAMERA SPECIFICATIONS

Price of the smartphone	600 US dollars
4K video recording	30 fps or 60 fps
Slow motion video	1080pixel at 240 fps
Super slow-motion	720pixel at 960 fps

After filming the video of the vibrating beam, the video is transferred to the Tracker software [13] in which the qualitative displacement of the beam edge at a small pixel inside the video is transformed into a quantitative displacement signal in the time domain as shown in Fig. 3. Fast Fourier Transform (FFT) was then implemented to the recovered time-domain displacement signal to obtain the modal frequencies which visualized as the peaks in the Fourier spectrum. Once the modal frequencies are determined, the motion magnification algorithm was utilized to extract the displacement at each of the recovered frequency to determine the mode shape. During processing, the displacement signal is filtered with a bandpass filter centered at each of the recovered model frequency. Therefore the two obtained processed videos represent the mode shapes at the first and second natural frequency. The obtained mode shapes in each of the processed video are transformed into quantitative data using Tracker.

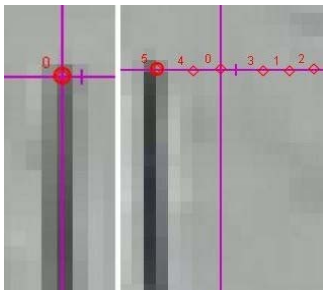

(a) (b)

Fig. 3 The first frame (a) and the fifth one (b) extracted using Tracker software [13] at a small pixel. Each number corresponds to the position of the beam at the specific frame

III. RESULTS AND DISCUSSIONS

A. Frequency Sensitivity and Modes

Fig. 4 shows the recovered displacement signal in the time domain. The Fourier spectrum of this displacement signal is shown in Fig. 5. Two peaks can be observed in this figure, which correspond to the first and second natural frequencies of the beam. The recovered first peak at 4.787 Hz with more power corresponds to the fundamental beam frequency, while

the second peak at 31.137 Hz corresponds to the second mode of the beam. Different modes of vibration do not equally contribute to the response of a structure. Thus, more energy is stored in the lower frequency modes. Table III compares the experimental and analytical results of the first two natural frequencies of the beam.

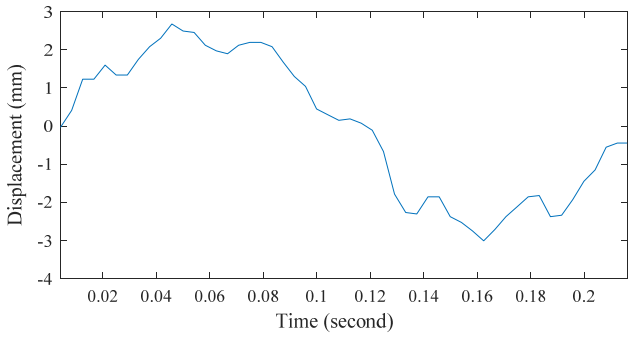

Fig. 4 Recovered displacement signal at the beam edge

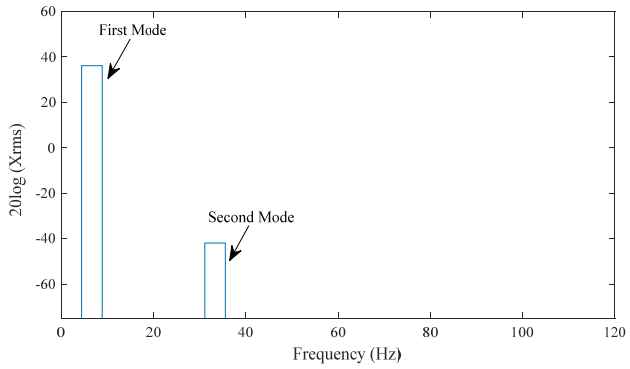

Fig. 5 Fourier spectrum of the time domain displacement signal

TABLE III
FIRST-TWO BEAM NATURAL FREQUENCIES USING DIFFERENT APPROACHES

Mode number	Experimental	Analytical	% Error
Frequency of first mode (Hz)	4.787	4.777	0.2%
Frequency of second mode (Hz)	31.137	29.94	3.84%

Based on Table III, it can be observed that the first two natural frequencies recovered from motion magnification technique are very close to the analytical approach. For the first mode, the difference between the experimental and analytical computation is only 0.01 Hz while it is 1.197 Hz for the second mode. However, the relative errors between the two approaches are respectively 0.2% and 3.84% for the first and second natural frequency. This small variation between different approaches is possible, due to the material variability such as the elastic modulus and density.

B. Mode Shape Analysis

The extraction of the displacements from the processed video at each natural frequency allows determining the mode shape. The objective was accomplished by controlling the low and high cut-off frequencies of the processed video. Figs. 6 and 7 show the analytical and experimental computation of the first and second mode shape of the beam, respectively.

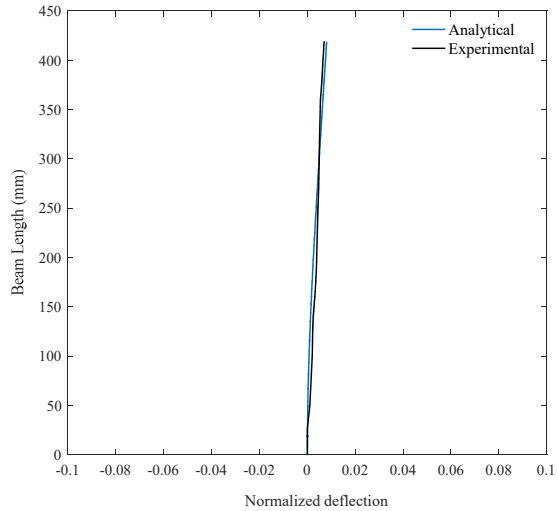

Fig. 6 First mode shape calculated using different approaches

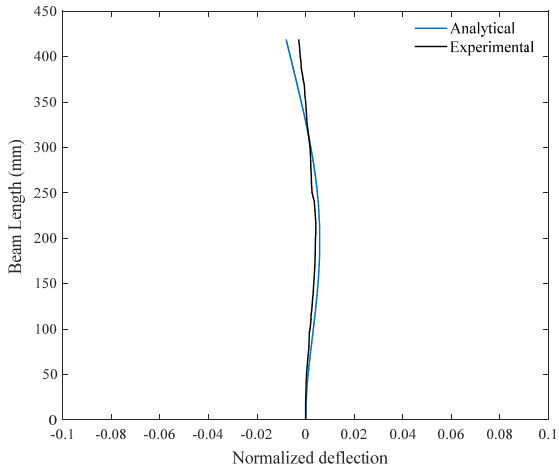

Fig. 7 Second mode shape calculated using different approaches

Based on Figs. 6 and 7, it can be observed that the experimental mode shapes are very close to the analytical ones. The similarity of mode shapes between different approaches can be examined based on MAC [14]. The MAC values vary between 0 and 1, where a value of 1 means a perfect match. A MAC value less than 0.77 indicates an unfortunate resemblance of mode shapes. The MAC value of a mode shape is essentially the normalized dot product of the modal vector at each common node (i.e., points), as presented in (8):

$$MAC = \frac{(\phi_i \cdot \phi_j)^2}{(\phi_i \cdot \phi_i) \times (\phi_j \cdot \phi_j)} \tag{8}$$

where $\emptyset_i$ and $\emptyset_j$ represent the modal vectors identified using different techniques.

The computed MAC values between the analytical and experimental approaches for the first and second mode shape are 0.9476 and 0.9048 respectively. Based on the MAC values and Figs. 6 and 7, it is observed that the first mode shape

achieves a better similarity between the two approaches than the second one. However, a consistent correspondence of the mode shapes extracted using different techniques is concluded.

IV. Conclusion

This paper proved the ability to recover the vibration behavior of a mechanical structure such as a cantilever beam using an inexpensive camera based on motion magnification technique. The relative error between the experimental and analytical approaches is below 4% for the first two natural frequencies of a cantilever beam. Besides, the first two-mode shapes were recovered with a MAC value of above 0.9 between the two approaches. Thus, this small error between the experimental and analytical techniques ensures the feasibility of an inexpensive smartphone camera as a non-contact vibration sensor.

Although the presented inexpensive experimental method is limited to relatively low frequencies with less than 120 Hz for a 240 fps camera (or less than 480 Hz for a 960 fps); however, this does not prevent the exploitation of this method and draws attention to large structures due to their low natural resonance frequencies. For future work, one can develop the algorithm of the method to an application for a smartphone, and the ability to visualize the vibration modes (model frequencies and mode shapes) of a vibrating structure. Besides, further studies can be conducted to utilize it for identification of the early damage detection in structures.

References

[1] T. Kranjc, J. Slavič, and M. Boltežar, "A comparison of strain and classic experimental modal analysis," Journal of Vibration and Control, vol. 22, no. 2, pp. 371–381, 2014.

[2] D. Mandal, D. Wadadar, and S. Banerjee, "Performance evaluation of damage detection algorithms for identification of debond in stiffened metallic plates using a scanning laser vibrometer," Journal of Vibration and Control, vol. 24, no. 12, pp. 2464–2482, 2018.

[3] K. Saravanan, A. Sekhar, "Crack detection in a rotor by operational deflection shape and kurtosis using laser vibrometer measurements," Journal of Vibration and Control, vol. 19, no. 8, pp. 1227–1239, 2013.

[4] J. Chen, N. Wadhwa, Y. Cha Y., F. Durand, W. Freeman, O. Buyukozturk. "Structural Modal Identification Through High Speed Camera Video: Motion Magnification," in 2014 Proc. of the Society for Experimental Mechanics Series Conf., pp. 191–197.

[5] D. Feng, M. Feng, "Identification of structural stiffness and excitation forces in time domain using noncontact vision-based displacement measurement," Journal of Sound and Vibration, vol. 406, pp. 15-28, 2017.

[6] J. Chen, N. Wadhwa, Y. Cha, F. Durand, W. Freeman, O. Buyukozturk, "Modal identification of simple structures with high-speed video using motion magnification," Journal of Sound and Vibration, vol. 345, pp: 58–71, 2015.

[7] P. Poozesh, A. Sarrafi, Z. Mao, P. Avitabile, C. Niezrecki, "Feasibility of extracting operating shapes using phase-based motion magnification technique and stereo-photogrammetry," Journal of Sound and Vibration, vol. 407, pp. 350–366, 2017.

[8] Video magnification. http://people.csail.mit.edu/mrub/vidmag/ (accessed 01.12.18).

[9] A. Davis, K. Bouman, J. Chen, M. Rubinstein, F. Durand, W. Freeman, "Visual vibrometry: Estimating material properties from small motion in video," in 2015 Proc. of the IEEE on Computer Vision and Pattern Recognition Conf., pp. 5335–5343.

[10] A. Sarrafi, Z. Mao, C. Niezrecki, P. Poozesh, "Vibration-based damage detection in wind turbine blades using Phase-based Motion Estimation and motion magnification," Journal of Sound and Vibration, vol. 421, pp. 300–318, 2018.

[11] A. Davis, M. Rubinstein, N. Wadhwa, G. Mysore, F. Durand, W. Freeman, "The visual microphone: passive recovery of sound from video," ACM T Graphic 2014; vol. 33(4): 10 pages.

[12] G. Balakrishnan, F. Durand, J. Guttag, "Detecting pulse from head motions in video," in 2013 Proc. of the IEEE on Computer Vision and Pattern Recognition Conf., pp. 3430–3437.

[13] Tracker. https://physlets.org/tracker/ (accessed 01.12.18).

[14] D. Ewins, "Modal testing: theory, practice, and application (2nd Ed)," Research Studies Press, Baldock, Hertfordshire, England, 2000; Philadelphia, PA.

[15] D. J. Inman. Engineering vibration. 3rd edition, 2007.

[16] N. Wadhwa, M. Rubinstein, F. Durand, WT. Freeman, "Phase-based video motion processing," ACM Trans. Graph., vol. 32, no. 4, 2013.

[17] D. Fleet, A. Jepson, "Computation of component image velocity from local phase information". International Journal of Computer Vision, vol. 5, no. 1, pp. 77–104, 1990.

[18] T. Gautama, M. Hulle, "A phase-based approach to the estimation of the optical flow field using spatial filtering," IEEE Trans Neural Network, vol. 13, no. 5, pp. 1127–1136, 2002.

[19] W. Freeman, E. Adelson, "The design and use of steerable filters," IEEE Trans Pattern Anal Mach Intell., vol. 13, no. 9, pp. 891–906, 1991.